

## Electrochemical Synthesis of ZnO Nanoparticles

Maria Starowicz\*<sup>[a]</sup> and Barbara Stypuła<sup>[a]</sup>

**Keywords:** Zinc / Nanostructures / Alcohols / Electrochemistry

The anodic behaviour of zinc was investigated in ethanol solution containing LiCl and water. Zinc was polarised by using cyclic voltammetry and chronoamperometry techniques. During the course of the dissolution of zinc, a colloidal suspension of ZnO nanoparticles was obtained in 0.1 M LiCl/ethanol solutions that contain H<sub>2</sub>O. The suspension is formed only if water is present, and the rate of the process depends on the water content. Moreover, the concentration

of H<sub>2</sub>O directly influences the size of the particles. However, there is evidence of a Zn<sub>5</sub>(OH)<sub>8</sub>Cl<sub>2</sub>·H<sub>2</sub>O admixture, which is detectable in the precipitates obtained with a high concentration of water. Polarisation of zinc under the given conditions is a very simple method of producing ZnO nanoparticles.

(© Wiley-VCH Verlag GmbH & Co. KGaA, 69451 Weinheim, Germany, 2008)

### Introduction

The interesting properties of zinc oxide have attracted the attention of many researchers in recent times. This wide band-gap semiconductor may have numerous possible applications, particularly in the form of thin films, nanowires, nanorods or nanoparticles. It can be used in optoelectronic and electronic devices,<sup>[1]</sup> as well as in the field of electrochemistry for the production of chemical sensors,<sup>[2]</sup> photocatalysts<sup>[3]</sup> and solar cells.<sup>[4]</sup> Very transparent ultrafine particles of ZnO are used in the production of sunscreens, paints, varnishes, plastics and cosmetics, especially for the blocking of broad UV-A and UV-B rays.

The microstructure and chemical properties of ZnO powders depend on the way in which they are synthesised. Until now, various techniques have been used for the preparation of ZnO particles, e.g. high-temperature hydrothermal synthesis,<sup>[5–7]</sup> laser heating<sup>[8]</sup> or the high-temperature decomposition method.<sup>[9]</sup> However, the high-temperature methods are unfavourable because of high energy consumption. In contrast to these processes, the solution-based route has recently stimulated wide interest<sup>[10–13]</sup> because of the low temperatures needed and the large-scale production of nanocrystalline ZnO. Electrochemical methods have also been employed in the synthesis of ZnO nanoparticles or films.<sup>[14–18]</sup>

Numerous electrochemical studies of Zn in both aqueous<sup>[19]</sup> and nonaqueous<sup>[20–22]</sup> environments have been performed because of the interest in Zn corrosion. Different

proposed mechanisms<sup>[20,21,23]</sup> assume that Zn is dissolved in a two-step process [Equation (1) and Equation (2)].



where Zn<sup>+</sup><sub>ads</sub> as an intermediate product, is adsorbed on the metal surface. It is known that the intermediate product is more stable in anhydrous, organic environments.

This paper presents the electrochemical studies of Zn in a solution of LiCl in ethanol. The addition of water leads to the synthesis of ZnO nanoparticles, the size of which can be controlled by the water content.

### Results and Discussion

Cyclic voltammetric investigations of zinc were first performed in a LiCl/C<sub>2</sub>H<sub>5</sub>OH electrolyte. The anodic polarisation curves were recorded for solutions with different concentrations of Cl<sup>–</sup> ions, and the results are presented in the Figure 1. From the curves obtained, one can distinguish the first oxidation and the limiting current region (region I: below –1.0 V) and the second oxidation and the active dissolution region (region II: above –1.0 V).

The shape of the anodic curves is in agreement with the general model, which is based on a two consecutive step mechanism [Equations (1) and (2)]. The first oxidation of Zn according to Equation (1) is visible as a hump below –1.0 V. The anodic dissolution of zinc proceeds intensively in region II, above –1.0 V, and coincides with the oxidation of Zn<sup>I</sup> to Zn<sup>II</sup> and with the formation of soluble complexes formed by the coordination of anions (X<sup>–</sup>) or ethoxy groups according to the following reactions [Equation (3) and Equation (4)].

[a] AGH – University of Science and Technology, Faculty of Foundry Engineering, Department of Chemistry and Corrosion of Metals  
Reymonta 23, 30-059 Krakow, Poland  
Fax: +48-12-6336348  
E-mail: mariast@agh.edu.pl

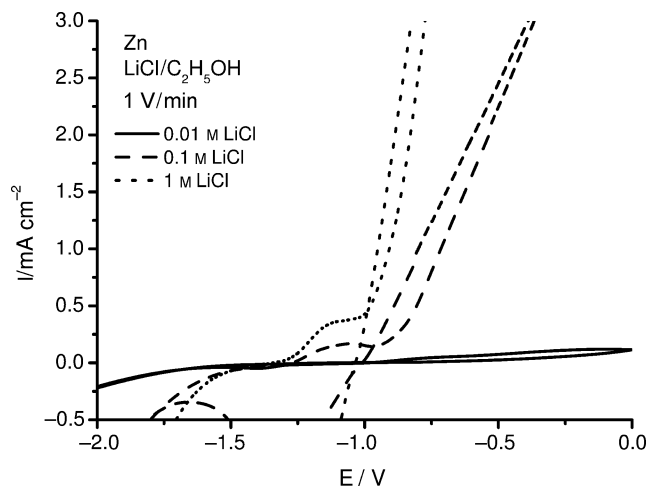
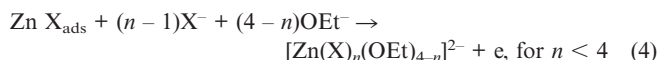
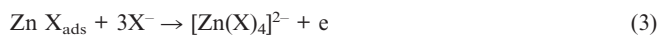


Figure 1. Polarisation curves of Zn obtained for different concentrations of LiCl in C<sub>2</sub>H<sub>5</sub>OH.



Sparingly soluble Zn<sup>I</sup> salts, formed at the initial stage, are introduced into the solution at potentials higher than −1.0 V as easily soluble [ZnCl<sub>4</sub>]<sup>2−</sup><sub>sol</sub> or [Zn(Cl)<sub>*n*</sub>(OEt)<sub>4−*n*</sub>]<sup>2−</sup><sub>sol</sub> complexes. After a longer polarisation time, the anodic surface has visible traces of etching.

The influence of water on the anodic polarisation of zinc in 0.1 M LiCl/C<sub>2</sub>H<sub>5</sub>OH solution was also investigated. The studies were performed with 0.1 M LiCl solutions with 1%, 3%, 5% and 50% distilled water in ethanol, as well as with 0.1 M LiCl in pure ethanol and pure distilled water. The cyclic voltammetric results are shown in the Figure 2. The addition of water causes a slight increase in the anodic current density in region I and initiates the dissolution of zinc in this region. The Zn<sup>I</sup> intermediate product is known to have a reduced stability in the presence of water.<sup>[20]</sup> The effect of water on the anodic dissolution process in region II is weak. However, there is a change in the coordination sphere of the anodic products in the presence of water.

Chronoamperometric polarisation was performed at potentials of −0.6 V and −0.4 V for a series of electrolytes, which were anhydrous or contained ethanol with 1%, 3%, 5% and 50% water. Finally, a solution of 0.1 M LiCl in distilled water was investigated. For the anhydrous solution, no precipitate was observed over 4 h of polarisation. In contrast, the solution of ethanol with 3% water started to lose transparency after about 40 min of polarisation at a potential of −0.6 V. It then turned into a white colloidal suspension. We stopped the process after 4 h of polarisation. The suspension was kept for 1 to 3 d, after which a white sediment precipitated. Chronoamperometric polarisation at −0.4 V resulted in a faster dissolution process, the first signs were already visible after 30 min.

The chemical composition of the obtained sediment was determined by means of energy dispersive X-ray analysis

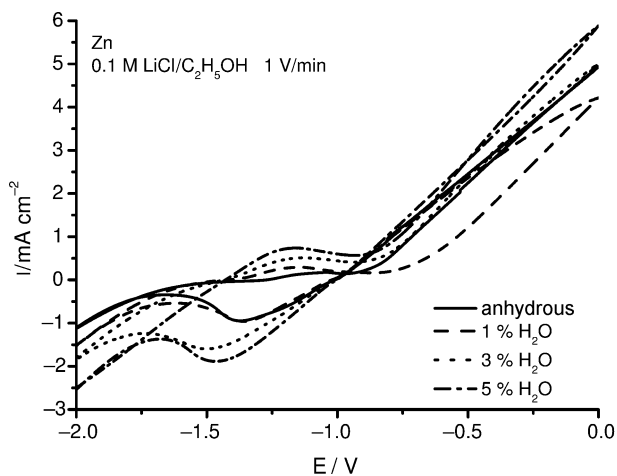


Figure 2. Influence of the concentration of water in 0.1 M LiCl/C<sub>2</sub>H<sub>5</sub>OH solutions on the Zn polarisation curves.

(EDX) and X-ray diffraction. EDX studies indicated the presence of Zn, O, C and Cl. The concentration of Cl that was present in the solution decreased after rinsing in ethanol. A sample EDX study for the rinsed precipitate obtained at a polarisation at −0.6 V for the solution containing 50% H<sub>2</sub>O revealed the following molar concentrations of substances: (36.8 ± 3.2)% Zn, (59.2 ± 1.6)% O and (3.9 ± 0.37)% Cl. X-ray diffraction studies (Figure 3) showed that for low concentrations of water (3%) ZnO<sup>[24]</sup> is obtained. At this H<sub>2</sub>O concentration, there is no clear evidence of any spurious phase. In the case of high water concentrations (50%), in addition to ZnO, another compound was detected and identified as Zn<sub>5</sub>(OH)<sub>8</sub>Cl<sub>2</sub>·H<sub>2</sub>O, simonkolleite.<sup>[25]</sup> It is noteworthy that the diffraction peaks for the samples with low concentrations of H<sub>2</sub>O are clearly wider, which provides evidence for the presence of small

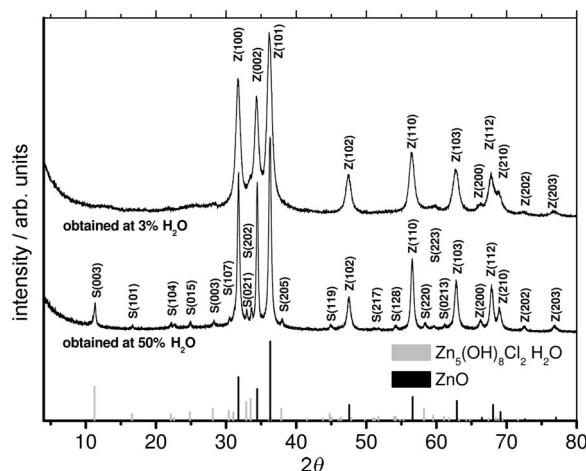


Figure 3. X-ray diffraction patterns recorded with Cu-K<sub>α</sub> radiation (λ = 1.54051 Å) for the precipitates obtained in the polarisation at −0.6 V. The solutions contained 3% and 50% H<sub>2</sub>O. Standard peak positions, intensities and indices are marked with black bars and Z(hkl) for ZnO and with grey bars and S(hkl) for Zn<sub>5</sub>(OH)<sub>8</sub>Cl<sub>2</sub>·H<sub>2</sub>O (simonkolleite).

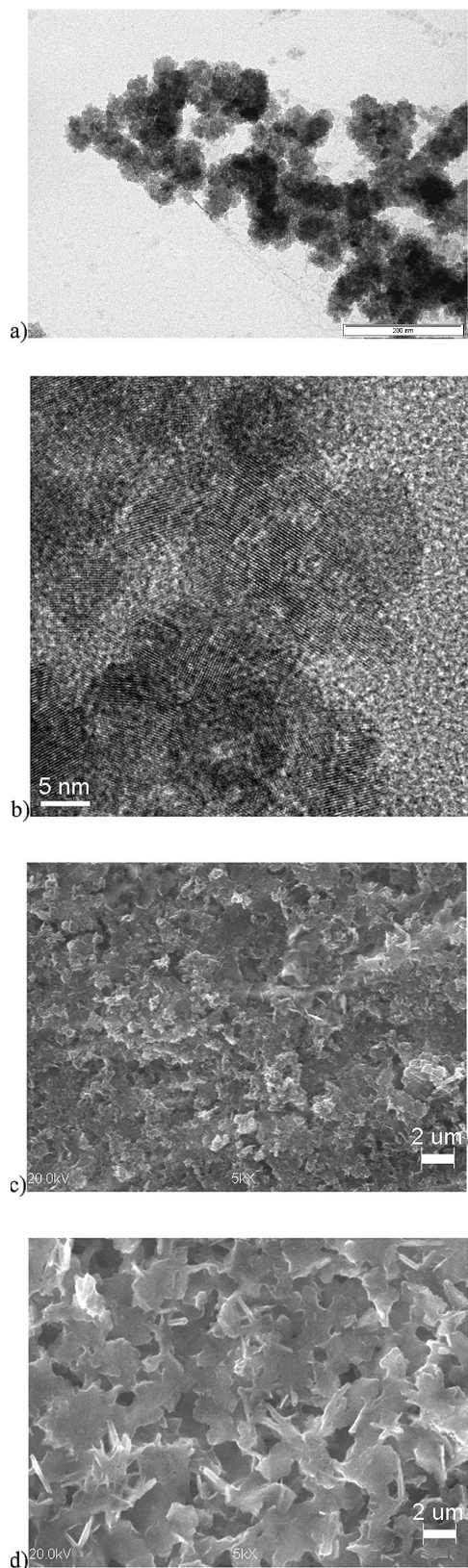
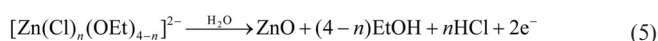


Figure 4. Morphology of the sediment obtained at  $-0.6$  V, (a) investigated by TEM for the 1%  $\text{H}_2\text{O}$  sample, (b) HRTEM for the 5%  $\text{H}_2\text{O}$  sample, (c) SEM for the 50%  $\text{H}_2\text{O}$  sample and (d) SEM for the pure water solution.

particles in the sediment. The wavy background may also be a symptom of very small precipitates.

Finally, we showed that the size of the produced particles can be controlled by the water content in the solution. For smaller concentrations of water, not only is the process slower, but also the size of the obtained particles is smaller. Figure 4 presents the SEM and TEM micrographs of the morphology of the sediment prepared at  $-0.6$  V. For the solutions that contained smaller amounts of water (1%, 3% or 5%), smaller nanoparticles were formed, which were observed by TEM or high resolution TEM (HRTEM) (Figure 4a and b) but were too small to be visible by lower resolution SEM. Figure 4b indicates that the size of the particles is roughly estimated to be between 5 and 20 nm. In Figure 4b, atomic rows are visible, which indicates the different orientations of the grains. The TEM figures do not show clearly that the particles are larger for the 5%  $\text{H}_2\text{O}$  samples than for the 3% and 1%  $\text{H}_2\text{O}$  samples; however, it was noticed that the precipitation of the sediment occurred at a faster rate for the 5%  $\text{H}_2\text{O}$  sample, which indicates the larger average size of the grains. For the samples with higher water content (Figure 4c and d), the particles become considerably larger and are characterised by platelike shapes. The SEM micrographs reveal that the particle size for the 50% water sample is of the order of  $1\text{ }\mu\text{m}$ , but for the pure water solution, the grains are already a few micrometers in size.

The fact that the observed process is realised uniquely with a presence of water implies that water plays a special role here. Hence, the following mechanism may be suggested. The anodic products –  $\text{Zn}^{\text{II}}$  chloride or alkoxide compounds – should undergo hydrolysis in the presence of water according to the following reaction [Equation (5)], which leads to the formation of ZnO nanoparticles.



Another process that occurs in our experiment is the formation of  $\text{Zn}_5(\text{OH})_8\text{Cl}_2 \cdot \text{H}_2\text{O}$ , simonkolleite, which is well evidenced at high water concentrations. This compound may be synthesised in the presence of water,  $\text{Zn}^{2+}$  or  $\text{ZnO}$  and  $\text{Cl}^-$ .<sup>[26,27]</sup>

## Conclusions

Potentiodynamic studies were performed on zinc, which undergoes aggressive anodic dissolution in ethanol solutions of LiCl salts in high potential regions (above  $-1.0$  V). Zinc oxide nanoparticles are formed in a  $0.1\text{ M}$  LiCl solution of ethanol containing water. The water concentration directly influences the rate of the process and determines the size of the produced nanoparticles. In addition, for higher water contents, there is evidence of a  $\text{Zn}_5(\text{OH})_8\text{Cl}_2 \cdot \text{H}_2\text{O}$  admixture in the sediment.

## Experimental Section

Lithium chloride ( $\text{LiCl} \geq 99.0\%$ ) was produced by Merck, anhydrous ethanol (99.8%) from EUROCHEM BGD. The reagents were used as received, without further purification. The disc-shaped electrode was prepared from metallic zinc of purity 99.99% and embedded in Teflon. The working surface was  $0.5 \text{ cm}^2$ . Samples were polished progressively from a 600 grit finish to a 1200 grit paper. Before electrochemical treatment, the electrodes were cleaned in anhydrous ethanol. Electrochemical measurements were performed in a one-compartment glass electrochemical cell. The experiment was performed under pure argon at room temperature. The applied three-electrode system consisted of a zinc disc as the working electrode, a platinum plate as the counter-electrode and  $\text{Ag}/\text{AgCl}$  as a reference electrode. The values of the potential given in this article refer to the  $\text{Ag}/\text{AgCl}$  electrode. The anodic properties of zinc were investigated by using PGZ301 Voltalab potentiostat by means of the potentiostatic and potentiodynamic technique. Potentiodynamic polarisation sweeps of the working electrode were realised at a rate of  $1.0 \text{ V/min}$ . Potentiostatic studies were performed at  $-0.6 \text{ V}$  and  $-0.4 \text{ V}$  for 4 h. The investigations on the size, morphology and composition of the obtained nanoparticles were realised by means of TEM, EDX and electron diffraction by using a Phillips CM20 TWIN microscope operating at  $200 \text{ kV}$ . SEM studies were performed with a JEOL 5500 LV instrument. X-ray diffraction of a precipitate was performed by means of a PANalytical X'Pert PRO diffractometer with the wavelength  $\lambda = 1.54051 \text{ \AA}$  of  $\text{Cu-K}_\alpha$  radiation.

## Acknowledgments

This work was financed by the Ministry of Science and Higher Education of Poland under the project number 3 T08C 011 30.

- [1] M. H. Huang, Y. Wu, H. Feick, N. Tran, E. Weber, P. Yang, *Adv. Mater.* **2001**, *13*, 113.
- [2] S. S. Weissenrieder, J. Müller, *Thin Solid Films* **1997**, *300*, 30.
- [3] M. Anpo, K. Chiba, M. Tomonari, S. Coluccia, M. Che, M. A. Fox, *Bull. Chem. Soc. Jpn.* **1991**, *64*, 543.
- [4] T. Yoshida, K. Terada, D. Schlettwein, T. Oekermann, T. Sugura, H. Minoura, *Adv. Mater.* **2000**, *12*, 1214.
- [5] R. Viswanathan, R. B. Gupta, *J. Supercrit. Fluids* **2003**, *27*, 187.
- [6] B. Baruwati, D. K. Kumar, S. V. Manorama, *Sens. Actuators, B* **2006**, *119*, 676.
- [7] S. Musić, D. Dragčević, S. Popović, M. Invanda, *Mater. Lett.* **2005**, *59*, 2388.
- [8] R. Wu, C. S. Xie, H. Xia, J. H. Hu, A. H. Wang, *J. Cryst. Growth* **2000**, *217*, 274.
- [9] K. G. Kanade, B. B. Kale, R. C. Aiyer, B. K. Das, *Mater. Res. Bull.* **2006**, *41*, 590.
- [10] L. Poul, S. Ammar, N. Jouini, F. Fievet, F. Villain, *J. Sol-Gel Sci. Technol.* **2003**, *26*, 261.
- [11] E. J. Hosono, S. Fujihara, T. Kimura, H. Imai, *J. Sol-Gel Sci. Technol.* **2004**, *29*, 1528.
- [12] C.-H. Hung, W.-T. Whang, *Mater. Chem. Phys.* **2003**, *82*, 705.
- [13] H. Wang, C. Xie, D. Zeng, *J. Cryst. Growth* **2005**, *277*, 372.
- [14] G. S. Huang, X. L. Wu, Y. C. Cheng, J. C. Shen, A. P. Huang, P. K. Chu, *Appl. Phys. A* **2007**, *86*, 463.
- [15] K. L. Levine, J. O. Iroh, P. B. Kosel, *Appl. Surf. Sci.* **2004**, *230*, 24.
- [16] H. Li, R. Wang, Ch. Guo, H. Zhang, *Mater. Sci. Eng. B* **2003**, *103*, 285.
- [17] G. Zhao, J.-J. Xu, H.-Y. Chen, *Anal. Biochem.* **2006**, *350*, 145.
- [18] Y.-F. Gao, M. Nagai, Y. Masuda, F. Sato, K. Koumoto, *J. Cryst. Growth* **2006**, *286*, 445.
- [19] X. G. Zhang, *Corrosion and Electrochemistry of Zinc*, Plenum Press, New York, **1996**.
- [20] J. Światowska-Mrowiecka, J. Banaś, *Electrochim. Acta* **2005**, *50*, 1829.
- [21] S. Białożor, E. T. Bandura, *Electrochim. Acta* **1987**, *37*, 891.
- [22] U. Lechner-Knoblach, E. Heitz, *Electrochim. Acta* **1987**, *32*, 901.
- [23] C. Cachet, F. Ganne, G. Maurin, J. Petitjean, V. Vivier, R. Wiart, *Electrochim. Acta* **2001**, *47*, 509.
- [24] Y. Dai, Y. Zhang, Z. L. Wang, *Solid State Commun.* **2003**, *126*, 629.
- [25] F. C. Hawthorne, E. Sokolova, *Can. Mineral.* **2002**, *40*, 939.
- [26] Q. Qu, L. Li, W. Bai, C. Yan, C.-n. Cao, *Corros. Sci.* **2005**, *47*, 2832.
- [27] H. Tanaka, A. Fujioka, A. Futouy, K. Kandori, T. Ishikawa, *J. Solid State Chem.* **2007**, *180*, 2061.

Received: September 16, 2007

Published Online: December 14, 2007